Published in final edited form as:
Mol Cell. 2010 July 9; 39(1): 86–99. doi:10.1016/j.molcel.2010.06.012.

Dephosphorylation of F-BAR protein Cdc15 modulates its conformation and stimulates its scaffolding activity at the cell division site

Rachel H. Roberts-Galbraith[1], **Melanie D. Ohi**[2], **Bryan A. Ballif**[3,*], **Jun-Song Chen**[1,*], **Ian McLeod**[4,*], **W. Hayes McDonald**[4], **Steven P. Gygi**[3], **John R. Yates III**[4], and **Kathleen L. Gould**[1]

[1]Howard Hughes Medical Institute and Department of Cell and Developmental Biology, Vanderbilt University School of Medicine, Nashville, TN 37232

[2]Department of Cell and Developmental Biology, Vanderbilt University School of Medicine, Nashville, TN 37232

[3]Department of Cell Biology, Harvard Medical School, Boston, MA 02115

[4]Department of Chemical Physiology, The Scripps Research Institute, La Jolla, CA 92037

Summary

Cytokinesis in *Schizosaccharomyces pombe* requires the function of Cdc15, founding member of the *pombe cdc15* homology (PCH) family of proteins. As an early, abundant contractile ring component with multiple binding partners, Cdc15 plays a key role in organizing the ring. We demonstrate that Cdc15 phosphorylation at many sites generates a closed conformation, inhibits Cdc15 assembly at the division site in interphase, and precludes interaction of Cdc15 with its binding partners. Cdc15 dephosphorylation induces an open conformation, oligomerization, and scaffolding activity during mitosis. Cdc15 mutants with reduced phosphorylation precociously appear at the division site in filament-like structures and display increased association with protein partners and the membrane. Our results indicate that Cdc15 phosphoregulation impels both assembly and disassembly of the contractile apparatus and suggest a regulatory strategy that PCH family and BAR superfamily members might broadly employ to achieve temporal specificity in their roles as linkers between membrane and cytoskeleton.

Introduction

In order for a eukaryotic cell to divide, a cytokinetic apparatus forms perpendicular to the mitotic spindle. In animal cells and fungi, this cytokinetic apparatus takes the form of a dynamic, actomyosin-based contractile ring that interacts intimately with the cell cortex and constricts to physically divide one cell into two (for review, see Balasubramanian et al., 2004). As with division of genetic material during mitosis, precise regulation of cytokinesis

Phone: 615-343-9500 Fax: 615-343-0723 kathy.gould@vanderbilt.edu.
*These authors contributed equally to this work.

Additional methods in supplemental text.

ensures accurate inheritance of the genome and maintenance of ploidy in daughter cells; failure to properly complete cell division contributes to tumorigenesis (Fujiwara et al., 2005).

Schizosaccharomyces pombe undergo a stereotypical symmetric cell division using a core set of conserved proteins required for placement and formation of the contractile ring (for review, see Balasubramanian et al., 2004). The core division machinery in *S. pombe* includes: actin, formin Cdc12, anillin-like protein Mid1, type II myosin Myo2, myosin light chains Rlc1 and Cdc4, tropomyosin Cdc8, profilin Cdc3, IQGAP Rng2, and the founding member of the *pombe cdc15*-homology (PCH) family, Cdc15 (for review, see Wolfe and Gould, 2005), which are incorporated into the ring in a prescribed order (Wu et al., 2003). Observations of contractile ring assembly in wild type and mutant backgrounds have led to a mathematical model of contractile ring formation, in which Mid1-dependent nodes of contractile ring components coalesce upon mitotic entry (Vavylonis et al., 2008; Wu et al., 2006). In parallel, the septation initiation network (SIN) kinase cascade facilitates contractile ring formation in a Mid1-independent manner, possibly through Cdc15 recruitment (Hachet and Simanis, 2008; Huang et al., 2008; Roberts-Galbraith and Gould, 2008). Despite these working models, a mechanistic understanding of the protein-protein and protein-membrane interactions key to ring assembly is immature.

Cdc15 is the founding member of the *pombe cdc15* homology family of proteins (Lippincott and Li, 2000), which share a conserved domain architecture of an N-terminal, membrane-binding F-BAR domain (Itoh et al., 2005; Tsujita et al., 2006) and, for most family members, a C-terminal SH3 domain. PCH proteins link the cell membrane and cytoskeleton to support a variety of cellular events, including endocytosis, cell motility, and generation of neural processes (for review, see Chitu and Stanley, 2007). In *S. pombe*, Cdc15 arrives early in contractile ring formation, is one of the most abundant proteins at the contractile ring, and is essential for cytokinesis (Fankhauser et al., 1995; Wu et al., 2003; Wu and Pollard, 2005). Through its F-BAR domain, Cdc15 interacts with formin Cdc12 and type I myosin Myo1, recruiting them for medial F-actin nucleation (Carnahan and Gould, 2003). Cdc15 also stabilizes the contractile ring through SH3 domain-mediated interactions with C2-domain protein Fic1 and paxillin homolog Pxl1 (Roberts-Galbraith et al., 2009). Cdc15 phosphorylation status varies during the cell cycle (Fankhauser et al., 1995), with mitotic dephosphorylation partially dependent on the Cdc14-like phosphatase Clp1 (Clifford et al., 2008; Wachtler et al., 2006). Dephosphorylation of Cdc15 by Clp1 stabilizes its contractile ring localization (Clifford et al., 2008) through an unknown molecular mechanism.

In this work, we explored the mechanism by which phosphorylation controls Cdc15 function in cytokinesis. We report that Cdc15 phosphorylation prevents its interaction with cytokinetic proteins and cortical localization during interphase while dephosphorylation of Cdc15 permits protein-protein interactions specifically in mitosis. Control of Cdc15 binding potential appears to be mediated by dramatic conformational and oligomeric changes in the protein. In support of this mechanism, phosphosite-abolished Cdc15 mutants localize medially and bind partners precociously, while also displaying increased membrane association. Our results identify Cdc15 phosphoregulation as an important switch point in the assembly/disassembly of the *S. pombe* contractile ring. Furthermore, this study suggests a potential regulatory mechanism for the BAR superfamily of proteins that can be used quickly and reversibly to control their membrane-cytoskeleton bridging potential.

Results

Hypophosphorylated Cdc15 localizes to the contractile ring and interacts with binding partners

Cdc15 localizes to cell tips or at the contractile ring depending on cell cycle phase (Carnahan and Gould, 2003; Fankhauser et al., 1995 and Fig. 1A) and multiple Cdc15 phosphoisoforms exist (Fig. 1B). It was previously noted that Cdc15 dephosphorylation coincides temporally with actin ring formation (Fankhauser et al., 1995). Likewise, in cell cycle arrests, Cdc15 localization to the contractile ring correlated with the presence of a hypophosphorylated form that was not detected in G1 or G2 arrested cells (Fig. 1A–C). Additionally, Cdc15 intensity at the contractile ring increases during anaphase and septation (Supp. Fig. 1A), when Cdc15 phosphorylation is at its minimum (Fankhauser et al., 1995). These observations suggested that dephosphorylation might direct Cdc15 relocalization.

Cdc15 binds to formin Cdc12 and their recruitment to the division site is interdependent (Carnahan and Gould, 2003; Chang et al., 1997). To determine whether Cdc15 phosphorylation status modulates this interaction, cells were arrested in G2, released to the permissive temperature, and samples were collected periodically. Cell lysates were probed with recombinant, bead-bound MBP or MBP linked to a fragment of Cdc12 that binds Cdc15. MBP-Cdc12(aa1-764) pulled down hypophosphorylated, but not hyperphosphorylated, Cdc15 (Fig. 1D). Clp1 dephosphorylates Cdc15 *in vivo* and *in vitro* (Clifford et al., 2008; Wachtler et al., 2006), so we tested whether the Cdc12-Cdc15 interaction was reduced in *clp1*Δ cells, in which Cdc15 dephosphorylation is incomplete. While Cdc15 protein levels are two times higher in *clp1*Δ cells, Cdc12 pulls down only 27% as much Cdc15 in a similar block and release experiment (Supp. Fig. 1B). Decreased Cdc15-Cdc12 interaction might contribute to the higher dynamicity of Cdc15 in *clp1*Δ cells (Clifford et al., 2008).

We identified Cdc15 as a prominent hit in both Cyk3 and Rng2 tandem affinity purifications by mass spectrometry (Supp. Figs. 1C and 1D). Coimmunoprecipitation experiments validated that Cyk3 and Rng2 can associate with Cdc15, but only when it is in its dephosphorylated state in mitotically arrested cells (Supp. Figs. 1E and 1F). These data suggest that phosphoregulation of Cdc15 might control its interaction with multiple proteins at the ring.

To test whether Cdc15 phosphorylation status might directly modulate its protein-protein interactions, hyperphosphorylated Cdc15 was purified from G2-arrested cells and treated with buffer alone, phosphatase, or phosphatase with inhibitors (Fig. 1E). Whereas hyperphosphorylated Cdc15 did not interact with MBP-Cdc12(aa1-764), hypophosphorylated Cdc15 was able to do so (Fig. 1F), indicating that phosphorylation of Cdc15 directly inhibits its interaction with Cdc12.

F-BAR domains interact with lipid bilayers *in vitro* (Itoh et al., 2005; Tsujita et al., 2006), so we used membrane flotation to investigate whether Cdc15 association with the plasma membrane might be impacted by its phosphorylation. Using *cps1*-191 lysate, in which Cdc15 is primarily hypophosphorylated, 49.1% of Cdc15 was present in membrane fractions (Fig 1. G–H). In contrast, 24.1% of Cdc15 from *cdc25*-22 lysate floated in these fractions, indicating a correlation between Cdc15 phosphorylation status and membrane association.

Cdc15 undergoes a conformational change when dephosphorylated

F-BAR domains from FBP17, CIP4, and PACSIN exist as crescent-shaped, obligate dimers that form higher ordered structures both *in vivo* and *in vitro* (Frost et al., 2008; Shimada et al., 2007; Wang et al., 2009). We hypothesized that dephosphorylation might regulate

similar oligomerization of Cdc15, providing a mechanism for the cell cycle control of its scaffolding capacity. To test this possibility, we purified hyperphosphorylated, full-length Cdc15 and treated the protein with phosphatase or a buffer control (Fig. 2A). We then imaged the resulting hyper- and dephosphorylated forms of Cdc15 by negative stain electron microscopy (EM). In the hyperphosphorylated sample, only globular particles were observed (Fig. 2B). Upon dephosphorylation, undulating, filament-like structures were visualized (Fig. 2C); these structures were not detected in the hyperphosphorylated sample. The average periodicity of the crescent-shapes measured 30.1 nm and the structures have an approximate thickness of 9.6 nm, which is somewhat longer and thicker than the CIP4 and FBP17 F-BAR domains (22 nm and 2.7 nm respectively) (Shimada et al., 2007).

To examine whether the F-BAR domain of Cdc15 might contribute to the curved shapes observed in full-length Cdc15 structures, we purified the Cdc15 F-BAR (amino acids 19-295) from bacteria (Fig. 2D) and examined its structure by negative stain EM. Curved Cdc15 F-BAR domains measured 27.4 nm in length and formed undulating oligomeric chains (Fig. 2E) as observed in the full-length protein.

To more quantitatively assess the conformational and oligomeric changes associated with Cdc15 dephosphorylation, hyper- and hypophosphorylated Cdc15-TAP was purified from *cdc25*-22 and *cps1*-191 arrests, respectively and subjected to velocity sedimentation analytical ultracentrifugation. Hyperphosphorylated Cdc15 sedimented in two major peaks (s=6.8 and 10.2) that correspond to molecular weights of ~248 (dimeric) and 500 kDa (tetrameric) respectively (Fig. 2F), while the lowest peak is TEV from the purification (Fig. 2G). The frictional ratio of 1.3 indicates that hyperphosphorylated Cdc15 adopts a globular like shape. Hypophosphorylated Cdc15 also sedimented with two major peaks (s= 3.9 and 6.4) that correspond to molecular weights of ~240 and 520 kDa respectively. However, these peaks represent only ~40% of the protein (vs. ~80% for hyperphosphorylated Cdc15), with the remaining 60% of Cdc15 sedimenting as higher order oligomers. Additionally the frictional ratio of 2.1 indicates that the hypophosphorylated form of Cdc15 adopts a much more elongated shape than the hyperphosphorylated form (Fig. 2F).

Cdc15 phosphomutants act precociously in vivo

Based on the aforementioned data, we reasoned that a constitutively hypophosphorylated mutant of Cdc15 might localize to the division site prior to mitosis and/or interact with binding partners prematurely. To identify *in vivo* sites of Cdc15 phosphorylation, Cdc15 was purified (Supp. Fig. 2A) and analyzed by mass spectrometry. The complexity and number of Cdc15 phosphorylation sites prompted three complementary analyses to maximize coverage and improve detection. In total, 33–52 *in vivo* sites of phosphorylation were revealed (Supp. Table 1). To prioritize sites for mutagenesis studies, we considered the number of times each phosphosite was identified and agreement between datasets. We also considered the clustering of similar kinase consensus sites, based on the idea that several similar sites together might cooperate to affect regional charge (Moses et al., 2007). We focused on sites matching an RXXS consensus (Fig. 3A), based on our observation that the 14-3-3 protein Rad24 binds Cdc15 (Supp. Fig. 2B), that 14-3-3 proteins bind to RXXS motifs where the serine residue is phosphorylated (Yaffe et al., 1997), and that 8 of 10 RXXS sites in the C-terminus of Cdc15 are conserved in other *Schizosaccharomyces* species (data not shown). Because Cdc15 is a Clp1 target (Clifford et al., 2008) and activity of Cdc14 phosphatases is restricted to phosphorylated SP/TP sites (Gray et al., 2003), we also focused on sites fitting the SP/TP consensus (Fig. 3A). A number of sites not matching either consensus (Fig. 3A) were abundant in the mass spectrometry data sets and were mutated in conjunction with RXXS and SP/TP sites. The selected sites were mutated to alanine (to abolish phosphorylation) or aspartic acid (to mimic phosphorylation) and mutant *cdc15* genes were integrated at the endogenous locus. Each phosphomutant rescued *cdc15* function, though

some caused defects in morphology, including cell bulging or rounding (Supp. Fig. 2C–D). Importantly, mutation of the identified sites to alanine successfully reduced Cdc15 phosphorylation, though to varying degrees (Fig. 3B–C).

The subcellular localization of each mutant protein was examined by live cell imaging. Whereas wild type Cdc15 localizes in spots at cell tips during interphase, each alanine mutant localized aberrantly to cell middles (Fig. 4A, arrows and quantitation in Fig. 4B) and sometimes formed larger structures that appeared filamentous (Fig. 4A, asterisks), evoking the EM structures we detected upon Cdc15 dephosphorylation *in vitro* (Fig. 2C). The aspartic acid mutants localized like wild type Cdc15 (Fig. 4A). With greater numbers of alanine substitutions, the phenotypes became more penetrant (Fig. 4B). Unlike wildtype Cdc15, all alanine mutants displayed medial localization in a G2 arrest (Fig. 4A–B) that was confined to the cell cortex (Fig. 4C). Additionally, the intensity of Cdc15-GFP alanine mutants was significantly increased at the contractile ring in mitosis and at cell tips in interphase, while several aspartic acid mutants showed reduced localization to these sites (Fig. 4D). The increase in intensity of Cdc15 alanine mutants at the contractile ring coincided with a decrease in dynamicity (Supp. Fig. 2E).

We were interested in identifying factors that contributed to medial localization of Cdc15 phosphomutants in interphase. It was not dependent on Cdc15 binding partners Cdc12 or Rng2 or on positioning cues Mid1 or Tea4 (Supp. Fig 3A). Therefore, Cdc15(SP11A) medial localization occurs without the proteins that promote proper localization of wild type Cdc15 in mitosis. Removal of the SH3 domain of Cdc15 was also not sufficient to drive medial localization, ruling out autoinhibition by this domain (Supp. Fig. 3B).

We next asked whether Cdc15 alanine phosphomutants recruit Cdc15 binding partners to the cell middle. Cdc15 binding partners Fic1, Cyk3, and Myo1, which are normally restricted to cell tips during interphase, formed medial spots in G2-arrested *cdc15(SP11A)* or *cdc15(RXXS13A)* cells (Fig. 5A and Supp. Fig. 3C) and Cyk3 colocalized with Cdc15(SP11A) in these spots (Supp. Fig. 3D). Cdc12 accumulated in one or two obvious, medial spots in *cdc15(SP11A)* cells, whereas Cdc12 either is not visible or appears in a faint spot in G2-arrested *cdc15*$^{+}$ cells (Fig. 5A). While Rng2 signal is normally weak or absent during interphase, Rng2 spots became detectable in the presence of Cdc15(SP11A) (Fig. 5A). Pxl1, however, was not detected in medial structures (data not shown), probably because Pxl1 is present at low levels during G2 (Pinar et al., 2008).

We next asked whether Cdc15(SP11A) could recruit contractile ring components beyond its direct binding partners. Medial targeting of Myo2 is thought to be inhibited in interphase by its phosphorylation and/or dephosphorylation at separate sites (Motegi et al., 2004; Mulvihill et al., 2001). Therefore, it was surprising that both Myo2 and its light chain Rlc1 were recruited to a medial meshwork in G2-arrested *cdc15(SP11A) and cdc15(RXXS13A)* cells (Fig. 5B and Supp. Fig. 3C). Additionally, the actin patch protein coronin (Crn1) formed several medial spots (and one noticeably brighter spot) in the *cdc15(SP11A)* mutant (Fig. 5B). In contrast, several proteins that typically arrive late in cytokinesis were not recruited prematurely in the *cdc15(SP11A)* mutant, including F-BAR protein Imp2, cell wall enzyme Cps1, septin Spn3, and RhoGEF Rgf3 (Fig. 5B and data not shown). Anillin-like protein Mid1 normally localizes to the nucleus and nodes during late interphase and expression of *cdc15(SP11A)* did not alter this pattern (Fig. 5B). In all, with the exception of Mid1, Cdc15 promotes mislocalization of early but not late contractile ring components to ectopic medial spots in interphase.

We next tested whether these premature localization events were reflective of precocious biochemical associations. Whereas recombinant MBP-Cdc12(aa1-764) pulls down

hypophosphorylated Cdc15 from mitotic lysate (Fig. 1D), Cdc15(SP11A) but not Cdc15(SP11D) interacts with MBP-Cdc12(aa1-764) during interphase (Fig. 5C). Cdc15 aspartic acid mutants also show decreased association with Cdc12 in mitosis (Supp. Fig. 4A). Cyk3 and Rng2 normally coimmunoprecipitate Cdc15 from mitotic lysate (Supp. Fig. 1E–F), but can coimmunoprecipitate Cdc15 alanine mutants from interphase lysate (Fig. 5D and Supp. Fig. 4B). Reciprocally, Rad24, which typically binds hyperphosphorylated Cdc15 (Supp. Fig. 2B) does not bind either Cdc15(RXXS13A) or Cdc15(RXXS13D) (Supp. Fig. 4C), indicating that Rad24-binding RXXS phosphorylation sites have been abolished by these mutations and that phosphomimetic mutations do not permit Rad24 binding. Additionally, mutation of phosphorylation sites to alanine increases membrane association of Cdc15 while mutation of sites to aspartic acid decreases membrane association (Fig. 5E).

While Cdc15(SP11A) formed extensive medial structures prior to mitosis, no discernable rings appeared and we therefore suspected that F-actin rings themselves were not forming prematurely. To examine this, F-actin was visualized with phalloidin staining and with an F-actin-binding GFP-LifeAct construct (Riedl et al., 2008). Both methods revealed a wild-type F-actin pattern in the *cdc15(SP11A)* mutant with the exception of an increase in medially localized F-actin spots (Fig. 5F and Supp. Fig. 3E). However, no early contractile rings or cables were detected, suggesting that Cdc12 relocalizes but is not fully active in G2-arrested *cdc15(SP11A)* mutant cells.

Many PCH family members function in endocytosis (for review, see Chitu and Stanley, 2007), which in yeast is accompanied by F-actin patch formation (Huckaba et al., 2004). We investigated whether the medial F-actin spots seen in the *cdc15(SP11A)* mutant were inappropriate sites of endocytosis. Endocytosis occurred only at cell tips in *cdc25*-22 arrested cells, but medial endocytosis occurred in *cdc15(SP11A)* mutant cells, as determined by uptake of the dye FM4-64 (Fig. 5G). Dysregulated Cdc15 can thus initiate inappropriate medial endocytosis, as well as contractile ring component recruitment.

Genetic analysis of the phosphomutants suggested that both alanine and aspartic acid mutants adversely affect cytokinesis (Supp. Fig. 4D), so we used time lapse microscopy to examine the progression of cytokinesis. Normally, Cdc15-GFP appears at cell middles coincident with or slightly after spindle pole body (SPB) separation (Wu et al., 2003), observed by the SPB marker, Sid4-RFP (Fig. 6A–B). All Cdc15 alanine mutants localized to the medial region of the cell before SPB separation (Figure 6A–B) and, in general, most alanine and aspartic acid mutants displayed delays in cytokinesis as a whole (Supp. Fig. 4E). More specifically, ring formation was significantly slower in *cdc15(27A)* and *cdc15(27D)* mutants, though the delay in the *cdc15(27A)* mutant seems to be due to slow coalescence of many medial spots while the delay in *cdc15(27D)* cells seems to be caused by reduced appearance of Cdc15 at the cell middle (Fig. 6A, C–D). *cdc15(27A)* cells made up for this delay to initiate constriction with proper timing, but *cdc15(27D)* cells took significantly longer to initiate constriction after contractile rings were formed. Finally, constriction took significantly longer in both *cdc15(27A)* and *cdc15(27D)* mutants (Fig. 6C–D). In total, these data indicate that dysregulation of Cdc15 phosphorylation or dephosphorylation impacts the timing of cytokinesis.

Discussion

In this study, we investigated the mechanism by which Cdc15 phosphoregulation controls its function as an organizer of the contractile ring. We demonstrate that Cdc15 dephosphorylation *in vitro* and *in vivo* induces conformational and oligomeric state changes. Artificial hypophosphorylation of Cdc15 *in vivo* triggers the formation of elaborate, medial Cdc15 structures at the cortex, the assembly of an extensive set of protein-protein

interactions among early ring components, but not F-actin filaments typical of early ring formation. Importantly, removal of Cdc15 phosphorylation sites is also sufficient to drive medial endocytosis, a key event in eukaryotic cytokinesis (Montagnac et al., 2008). Constitutive Cdc15 hypophosphorylation stabilizes Cdc15 at the site of cell division in both interphase and mitosis, while phosphomimetic mutants diminish Cdc15 cortical localization. Phosphoregulation of protein conformation might be a general mechanism used by PCH family members or other relatives in the BAR superfamily to temporally restrict their availability as bridges between the membrane and cytoskeleton.

Phosphoregulation of Cdc15 structure and function

Isolated F-BAR domains form end-to-end oligomers vital to their function in binding and bending membranes (Frost et al., 2008; Shimada et al., 2007; Wang et al., 2009), and our EM results indicate that the isolated Cdc15 F-BAR domain behaves similarly (Fig. 2E). One EM study of a full-length, F-BAR protein was reported, but the hallmark curved F-BAR structure was not detected (Halbach et al., 2007). In contrast, our EM images of hypophosphorylated full-length Cdc15 are the first to reveal the expected crescent shape and repeating structures consistent with F-BAR domains. Our images also suggest that phosphorylation of the full-length protein limits oligomerization of the FBAR domain.

Many phosphorylation sites must be removed before Cdc15 activity becomes obviously uncoupled from normal cell cycle controls. Mutants with subsets of the alanine substitutions display mild phenotypes (Supp. Fig. 3F–G), while *cdc15(RXXS13A)* and *cdc15(SP11A)* mutants display a moderate phenotype and the *cdc15(27A)* mutant phenotype is most severe. Because preventing phosphorylation at either kinase consensus site results in similar phenotypes, we speculate that phosphorylation influences Cdc15 as an electrostatic threshold. Below this threshold, hypophosphorylated Cdc15 prefers an open protein conformation (Fig. 7A) that permits oligomerization, membrane binding, and protein-protein interactions at the contractile ring (Fig. 7B). The reverse likely occurs during ring constriction, with Cdc15 phosphorylation facilitating its clearance from the division site for ring disassembly. Consistent with this model, constitutively dephosphorylated Cdc15 impedes cytokinetic events in which remodeling is key—reorganization of nodes to form the ring and disassembly of the ring during constriction. Interestingly, Cdc15 intensity at the cell tips is also increased in alanine mutants and decreased in aspartic acid mutants, suggesting that a small population of Cdc15 molecules might be locally phosphoregulated during interphase at cell tips separate from bulk mitotic dephosphorylation.

Although the Cdc15 alanine mutants provided easily interpretable phenotypes, analysis of the aspartic acid mutants yielded ambiguous results. These mutations were meant to mimic the phosphorylated state, and while these Cdc15 mutants are clearly hypomorphic, our evidence suggests that we have not achieved a fully mimetic mutant. First, the RXXD mutants failed to bind Rad24 like hyperphosphorylated Cdc15 (Supp. Fig. 4C). Second, the aspartic acid mutations failed to recapitulate the higher Cdc15 dynamicity previously demonstrated for hyperphosphorylated Cdc15 in *clp1*Δ cells (Clifford et al., 2008 and Supp. Fig. 2E). Our model predicts that constitutively hyperphosphorylated Cdc15 would be lethal, locking Cdc15 into a “closed” conformation that is unable to bind its partners or localize to the contractile ring. It might not be possible to generate this form using phosphosite substitutions, and further experimentation will be required to test this hypothesis.

Nearly all of the phosphorylation sites targeted for mutagenesis in this study lie between the F-BAR and SH3 domains, in a large region of the protein predicted to be unstructured (data not shown and Dosztanyi et al., 2005). Intrinsically unstructured domains are more likely to be phosphorylated, are targeted by more protein kinases, and display lower conservation relative to globular domains (Gsponer et al., 2008). Phosphorylation might induce the Cdc15

unstructured region to interfere with F-BAR access to its binding partners or generate a bulk negative charge that binds basic residues important for F-BAR domain oligomerization or membrane association (Fig. 7A). Based on the number and diversity of phosphorylation sites within this region, we conclude that Cdc15 is targeted for regulation by several kinases and phosphatases and that Cdc15 phosphoregulation could be an integration point for multiple inputs that fine-tune the timing of cytokinesis. The variable size and composition of unstructured regions within the BAR superfamily might allow divergent BAR proteins to use phosphoregulation of conformation as a common regulatory strategy, with evolutionarily varied sites and regulators appropriate for different cellular contexts.

Step-wise assembly of the contractile ring

The *cdc15* alanine mutants are the first described mutants in *S. pombe* in which dysregulation of one contractile ring component triggers recruitment of other ring proteins and assembly of complexes at the cell middle prior to mitotic entry. However, these complexes do not form contractile rings, indicating that recruitment of Cdc12 formin and its activation are two separable events. The mechanism of Cdc12 activation remains undefined (Yonetani et al., 2008), but presumably one mode occurs downstream of SIN signaling, as SIN activation in G2 induces formation of contractile rings competent for constriction, with recruitment and activation of Cdc12 (Hachet and Simanis, 2008; Schmidt et al., 1997). Mid1, a key component of “nodes” that direct medial contractile ring placement (Wu et al., 2006), was not recruited to Cdc15(SP11A) assemblies, suggesting that it is also independently regulated. Thus, Cdc15 dephosphorylation is likely one of several key steps in formation of the contractile apparatus. We envision that the dysregulated Cdc15 mutants will provide useful genetic backgrounds for dissecting other regulatory events.

Phosphoregulation of BAR superfamily proteins

BAR proteins link the cytoskeleton to the cell membrane in the processes of endocytosis, cytokinesis, motility and neural morphogenesis (for reviews, see Chitu and Stanley, 2007; Ren et al., 2006), but a common mode of regulating these proteins has not been demonstrated. Phosphorylation has been reported for several PCH family members, including PACSIN/syndapin (Plomann et al., 1998), PSTPIP (Spencer et al., 1997), CIP4 (Larocca et al., 2004), and Hof1 (Vallen et al., 2000), and, more broadly, for a variety of BAR superfamily members (Bauerfeind et al., 1997; Lee et al., 1998; Wu et al., 2005). In budding yeast, where global phosphorylation data is most thorough, phosphorylation sites were identified on four of five F-BAR proteins and all three BAR domain proteins (Albuquerque et al., 2008; Chi et al., 2007; Li et al., 2007; Smolka et al., 2007). Importantly, in several cases, BAR protein phosphorylation inhibits protein-protein interactions (Bauerfeind et al., 1997; Floyd et al., 2001; Wu et al., 2005; Wu et al., 1998). Therefore, combinatorial phosphorylation could be a wide-ranging mechanism that influences the conformation, membrane binding capacity, and protein-protein interactions of BAR superfamily members, with a dynamic phosphorylation/dephosphorylation cycle controlling their functions during diverse biological processes.

Experimental procedures

Yeast strains, media, and genetic methods

Strains (Supp. Table 2) were grown in yeast extract (YE) media (Moreno et al., 1991) or 4× YE media for large-scale purifications. Arrests of temperature or cold sensitive mutants were achieved after 4 h at 36°C or 7 h at 18°C, except *cdc25*-22 arrests for imaging purposes were at 36°C for 2.5–3 h. For block and release experiments, cells were arrested at 36°C for 3.5 h and released to 25°C at the zero time point before sample collection. A lithium acetate protocol was used for all transformations of *S. pombe* cells (Keeney and Boeke, 1994).

For integration of *cdc15* mutants at the endogenous locus, *cdc15*Δ was rescued with pIRT2-*cdc15* constructs with 5' and 3' noncoding regions. Integrants resistant to 5-fluorourotic acid were isolated and verified by PCR. *cdc15*, *cdc15* mutants, *rng2*, *cyk3*, and *imp2* were tagged endogenously at their 3' termini (Bahler et al., 1998). Standard methods were used for strain construction and tetrad analysis.

Molecular biology methods

Phosphorylation site mutations were created in a pIRT2-*cdc15* integration vector (Roberts-Galbraith et al., 2009) using a QuikChange Site-Directed Mutagenesis kit or a QuikChange Multi-site Site-Directed Mutagenesis kit (Agilent Technologies) and all mutant vectors were sequenced to ensure that no other mutations were present in the *cdc15* coding region.

Protein Methods

Cell pellets were snap frozen and lysed by bead disruption in NP-40 lysis buffer as previously described (Gould et al., 1991), except that 0.5 mM diisopropyl fluorophosphate (Sigma-Aldrich) was added for all protein purifications from yeast. Immunoprecipitation experiments and western blot analyses were performed as previously described (Roberts-Galbraith et al., 2009). Alternatively, protein run on SDS-PAGE was detected with coomassie (Sigma) or silver staining (GE Healthcare). MBP-Cdc12(aa1-764) was produced and used for pull down experiments as previously described (Carnahan and Gould, 2003), except binding of this protein to purified Cdc15 was performed in the presence of 0.02 μg/μl bovine serum albumin (Sigma). His_6-Cdc15(F-BAR) (amino acids 19-295) was purified on His-Bind resin (Novagen) as per the manufacturer's protocol.

For all phosphatase treatments, purified or immunoprecipitated protein was incubated with lambda phosphatase (New England Biolabs) in 25 mM HEPES-NaOH pH 7.4, 150 mM NaCl, and 1 mM $MnCl_2$ for 40 minutes at 30°C. In samples with phosphatase plus inhibitors, 50 mM EDTA and 20 mM Na_3VO_4 were added.

Large scale protein purifications were performed in several ways. For Cdc12 *in vitro* binding experiments, lysates were prepared and cleared as previously described (Tasto et al., 2001). Cdc15-TEV2xProtA was isolated on tosylactivated Dynabeads (M280, Invitrogen) coated with rabbit IgG (MP Biomedicals). Beads were washed four times with NP-40 lysis buffer and twice with TEV cleavage buffer (10 mM Tris-HCl pH 8.0, 150 mM NaCl, 0.1% NP-40, 0.5 mM EDTA, and 1.0 mM DTT). Protein was cleaved from the beads with TEV protease (Invitrogen). For analytical ultracentrifugation experiments, TAP strains were used and the purifications were scaled up 4×. The same purification scheme was used for electron microscopy experiments, with two exceptions: the TEV cleavage buffer contained only 0.2% NP-40 and TEV was removed with a 100 MWCO Microcon column (Millipore) before phosphatase treatment.

Membrane flotation experiments were performed as previously described (Takeda et al., 2004), with the following modifications. 300 μl cleared lysate in TNE (50 mM Tris-HCl pH 7.4, 150 mM NaCl, 5 mM EDTA) was adjusted to 40% Optiprep (Sigma) and overlaid with 1.44 ml of 35% Optiprep in TNE and 240 μl of TNE alone. The resulting gradient was spun in an SW55Ti rotor at 200,000 g for 2 h at 4°C. Each gradient was divided into 6 fractions from top to bottom for immunoblotting.

Microscopy methods

Live cell imaging was done as previously described (Roberts-Galbraith et al., 2009), except that a 7–30% lactose gradient was used to synchronize cells before time lapse experiments. The 90° image rotation was created using Metamorph 7.1 software (MDS Analytical

Technologies). P values from FRAP analyses were calculated from best-fit curves in Prism 4.0c software (Graphpad Software, Inc.). Intensity quantitations were made with ImageJ software (http://rsbweb.nih.gov/ij/).

Fixation of cells for DAPI and methyl blue staining was performed as described (Roberts-Galbraith et al., 2009). Cells were fixed in formaldehyde and stained with Alexa Fluor 488-Phalloidin (Molecular Probes) as previously described (Pelham and Chang, 2001). For FM4-64 staining, arrested cells were quickly spun down and resuspended in warm YE with 0.05 mM FM4-64 (Molecular Probes) before immediate confocal imaging.

Electron microscopy

Uranyl formate stained samples were prepared for EM as described (Ohi et al., 2004). In brief, 2.5 μl of sample was absorbed to a glow discharged 200-mesh copper grid covered with carbon-coated collodion film. The grid was washed in two drops of water and then stained with two drops of uranyl formate (0.75%). Samples were imaged on a FEI Morgagni electron microscope operated at an acceleration voltage of 100 kV. Images were recorded at a magnification of 18–36,000× and collected using a 1K × 1K CCD camera (ATM).

Analytical Ultracentrifugation

Sedimentation velocity experiments were run at 30,000 RPM (4°C) on an Optima XLI (Beckman-Coulter, Fullerton, CA), with a 4-hole An60Ti rotor using double sector cells with charcoal- filled Epon centerpieces (path length 1.2 cm) and quartz windows. The velocity scans were analyzed with the program Sedfit (version 8.7) (Schuck, 2000) using 250 scans collected approximately 2 min apart. Size distributions were determined for a confidence level of $p = 0.95$, a resolution of $n = 200$, and sedimentation coefficients between 0 and 28 s.

Supplementary Material

Refer to Web version on PubMed Central for supplementary material.

Acknowledgments

We thank Curtis Thorne, Ben Wolfe, Jianqiu Wu, Scott Collier, the M. Ohi laboratory, and the VUMC Cell Imaging Shared Resource Core for technical assistance and Drs. Fred Chang, Dannel McCollum, Snezhana Oliferenko, and Kaoru Takegawa for sharing reagents. We are grateful to past and present members of the Gould laboratory for critically reading this manuscript and for helpful discussions.

R. H. R.-G. has been supported by the National Science Foundation fellowship DGE-0238741 and NIH grant GM068786. S.P.G. is supported by NIH grant HG003456. J.R.Y. is supported by NIH grant P41 RR011823. This work was supported by NIH grant GM068786 and the Howard Hughes Medical Institute, of which K.L.G. is an investigator.

References

Albuquerque CP, Smolka MB, Payne SH, Bafna V, Eng J, Zhou H. A multidimensional chromatography technology for in-depth phosphoproteome analysis. Mol Cell Proteomics 2008;7:1389–1396. [PubMed: 18407956]

Bahler J, Wu JQ, Longtine MS, Shah NG, McKenzie A 3rd, Steever AB, Wach A, Philippsen P, Pringle JR. Heterologous modules for efficient and versatile PCR-based gene targeting in Schizosaccharomyces pombe. Yeast 1998;14:943–951. [PubMed: 9717240]

Balasubramanian MK, Bi E, Glotzer M. Comparative analysis of cytokinesis in budding yeast, fission yeast and animal cells. Curr Biol 2004;14:R806–818. [PubMed: 15380095]

Bauerfeind R, Takei K, De Camilli P. Amphiphysin I is associated with coated endocytic intermediates and undergoes stimulation-dependent dephosphorylation in nerve terminals. J Biol Chem 1997;272:30984–30992. [PubMed: 9388246]

Carnahan RH, Gould KL. The PCH family protein, Cdc15p, recruits two F-actin nucleation pathways to coordinate cytokinetic actin ring formation in Schizosaccharomyces pombe. J Cell Biol 2003;162:851–862. [PubMed: 12939254]

Chang F, Drubin D, Nurse P. cdc12p, a protein required for cytokinesis in fission yeast, is a component of the cell division ring and interacts with profilin. J Cell Biol 1997;137:169–182. [PubMed: 9105045]

Chi A, Huttenhower C, Geer LY, Coon JJ, Syka JE, Bai DL, Shabanowitz J, Burke DJ, Troyanskaya OG, Hunt DF. Analysis of phosphorylation sites on proteins from Saccharomyces cerevisiae by electron transfer dissociation (ETD) mass spectrometry. Proc Natl Acad Sci U S A 2007;104:2193–2198. [PubMed: 17287358]

Chitu V, Stanley ER. Pombe Cdc15 homology (PCH) proteins: coordinators of membrane-cytoskeletal interactions. Trends Cell Biol 2007;17:145–156. [PubMed: 17296299]

Clifford DM, Wolfe BA, Roberts-Galbraith RH, McDonald WH, Yates JR 3rd, Gould KL. The Clp1/Cdc14 phosphatase contributes to the robustness of cytokinesis by association with anillin-related Mid1. J Cell Biol 2008;181:79–88. [PubMed: 18378776]

Dosztanyi Z, Csizmok V, Tompa P, Simon I. IUPred: web server for the prediction of intrinsically unstructured regions of proteins based on estimated energy content. Bioinformatics 2005;21:3433–3434. [PubMed: 15955779]

Fankhauser C, Reymond A, Cerutti L, Utzig S, Hofmann K, Simanis V. The S. pombe cdc15 gene is a key element in the reorganization of F-actin at mitosis. Cell 1995;82:435–444. [PubMed: 7634333]

Floyd SR, Porro EB, Slepnev VI, Ochoa GC, Tsai LH, De Camilli P. Amphiphysin 1 binds the cyclin-dependent kinase (cdk) 5 regulatory subunit p35 and is phosphorylated by cdk5 and cdc2. J Biol Chem 2001;276:8104–8110. [PubMed: 11113134]

Frost A, Perera R, Roux A, Spasov K, Destaing O, Egelman EH, De Camilli P, Unger VM. Structural basis of membrane invagination by F-BAR domains. Cell 2008;132:807–817. [PubMed: 18329367]

Fujiwara T, Bandi M, Nitta M, Ivanova EV, Bronson RT, Pellman D. Cytokinesis failure generating tetraploids promotes tumorigenesis in p53-null cells. Nature 2005;437:1043–1047. [PubMed: 16222300]

Gould KL, Moreno S, Owen DJ, Sazer S, Nurse P. Phosphorylation at Thr167 is required for Schizosaccharomyces pombe p34cdc2 function. Embo J 1991;10:3297–3309. [PubMed: 1655416]

Gray CH, Good VM, Tonks NK, Barford D. The structure of the cell cycle protein Cdc14 reveals a proline-directed protein phosphatase. Embo J 2003;22:3524–3535. [PubMed: 12853468]

Gsponer J, Futschik ME, Teichmann SA, Babu MM. Tight regulation of unstructured proteins: from transcript synthesis to protein degradation. Science 2008;322:1365–1368. [PubMed: 19039133]

Hachet O, Simanis V. Mid1p/anillin and the septation initiation network orchestrate contractile ring assembly for cytokinesis. Genes Dev 2008;22:3205–3216. [PubMed: 19056897]

Halbach A, Morgelin M, Baumgarten M, Milbrandt M, Paulsson M, Plomann M. PACSIN 1 forms tetramers via its N-terminal F-BAR domain. Febs J 2007;274:773–782. [PubMed: 17288557]

Huang Y, Yan H, Balasubramanian MK. Assembly of normal actomyosin rings in the absence of Mid1p and cortical nodes in fission yeast. J Cell Biol 2008;183:979–988. [PubMed: 19075108]

Huckaba TM, Gay AC, Pantalena LF, Yang HC, Pon LA. Live cell imaging of the assembly, disassembly, and actin cable-dependent movement of endosomes and actin patches in the budding yeast, Saccharomyces cerevisiae. J Cell Biol 2004;167:519–530. [PubMed: 15534003]

Itoh T, Erdmann KS, Roux A, Habermann B, Werner H, De Camilli P. Dynamin and the actin cytoskeleton cooperatively regulate plasma membrane invagination by BAR and F-BAR proteins. Dev Cell 2005;9:791–804. [PubMed: 16326391]

Keeney JB, Boeke JD. Efficient targeted integration at leu1-32 and ura4-294 in Schizosaccharomyces pombe. Genetics 1994;136:849–856. [PubMed: 8005439]

Larocca MC, Shanks RA, Tian L, Nelson DL, Stewart DM, Goldenring JR. AKAP350 interaction with cdc42 interacting protein 4 at the Golgi apparatus. Mol Biol Cell 2004;15:2771–2781. [PubMed: 15047863]

Lee J, Colwill K, Aneliunas V, Tennyson C, Moore L, Ho Y, Andrews B. Interaction of yeast Rvs167 and Pho85 cyclin-dependent kinase complexes may link the cell cycle to the actin cytoskeleton. Curr Biol 1998;8:1310–1321. [PubMed: 9843683]

Li X, Gerber SA, Rudner AD, Beausoleil SA, Haas W, Villen J, Elias JE, Gygi SP. Large-scale phosphorylation analysis of alpha-factor-arrested Saccharomyces cerevisiae. J Proteome Res 2007;6:1190–1197. [PubMed: 17330950]

Lippincott J, Li R. Involvement of PCH family proteins in cytokinesis and actin distribution. Microsc Res Tech 2000;49:168–172. [PubMed: 10816256]

Montagnac G, Echard A, Chavrier P. Endocytic traffic in animal cell cytokinesis. Curr Opin Cell Biol 2008;20:454–461. [PubMed: 18472411]

Moreno S, Klar A, Nurse P. Molecular genetic analysis of fission yeast Schizosaccharomyces pombe. Methods Enzymol 1991;194:795–823. [PubMed: 2005825]

Moses AM, Heriche JK, Durbin R. Clustering of phosphorylation site recognition motifs can be exploited to predict the targets of cyclin-dependent kinase. Genome Biol 2007;8:R23. [PubMed: 17316440]

Motegi F, Mishra M, Balasubramanian MK, Mabuchi I. Myosin-II reorganization during mitosis is controlled temporally by its dephosphorylation and spatially by Mid1 in fission yeast. J Cell Biol 2004;165:685–695. [PubMed: 15184401]

Mulvihill DP, Barretto C, Hyams JS. Localization of fission yeast type II myosin, Myo2, to the cytokinetic actin ring is regulated by phosphorylation of a C-terminal coiled-coil domain and requires a functional septation initiation network. Mol Biol Cell 2001;12:4044–4053. [PubMed: 11739799]

Ohi M, Li Y, Cheng Y, Walz T. Negative Staining and Image Classification - Powerful Tools in Modern Electron Microscopy. Biol Proced Online 2004;6:23–34. [PubMed: 15103397]

Pelham RJ Jr. Chang F. Role of actin polymerization and actin cables in actin-patch movement in Schizosaccharomyces pombe. Nat Cell Biol 2001;3:235–244. [PubMed: 11231572]

Pinar M, Coll PM, Rincon SA, Perez P. Schizosaccharomyces pombe Pxl1 is a Paxillin Homologue that Modulates Rho1 Activity and Participates in Cytokinesis. Mol Biol Cell. 2008

Plomann M, Lange R, Vopper G, Cremer H, Heinlein UA, Scheff S, Baldwin SA, Leitges M, Cramer M, Paulsson M, Barthels D. PACSIN, a brain protein that is upregulated upon differentiation into neuronal cells. Eur J Biochem 1998;256:201–211. [PubMed: 9746365]

Ren G, Vajjhala P, Lee JS, Winsor B, Munn AL. The BAR domain proteins: molding membranes in fission, fusion, and phagy. Microbiol Mol Biol Rev 2006;70:37–120. [PubMed: 16524918]

Riedl J, Crevenna AH, Kessenbrock K, Yu JH, Neukirchen D, Bista M, Bradke F, Jenne D, Holak TA, Werb Z, et al. Lifeact: a versatile marker to visualize F-actin. Nat Methods 2008;5:605–607. [PubMed: 18536722]

Roberts-Galbraith RH, Chen JS, Wang J, Gould KL. The SH3 domains of two PCH family members cooperate in assembly of the Schizosaccharomyces pombe contractile ring. J Cell Biol 2009;184:113–127. [PubMed: 19139265]

Roberts-Galbraith RH, Gould KL. Stepping into the ring: the SIN takes on contractile ring assembly. Genes Dev 2008;22:3082–3088. [PubMed: 19056889]

Schmidt S, Sohrmann M, Hofmann K, Woollard A, Simanis V. The Spg1p GTPase is an essential, dosage-dependent inducer of septum formation in Schizosaccharomyces pombe. Genes Dev 1997;11:1519–1534. [PubMed: 9203579]

Schuck P. Size-distribution analysis of macromolecules by sedimentation velocity ultracentrifugation and lamm equation modeling. Biophys J 2000;78:1606–1619. [PubMed: 10692345]

Shimada A, Niwa H, Tsujita K, Suetsugu S, Nitta K, Hanawa-Suetsugu K, Akasaka R, Nishino Y, Toyama M, Chen L, et al. Curved EFC/F-BAR-domain dimers are joined end to end into a filament for membrane invagination in endocytosis. Cell 2007;129:761–772. [PubMed: 17512409]

Smolka MB, Albuquerque CP, Chen SH, Zhou H. Proteome-wide identification of in vivo targets of DNA damage checkpoint kinases. Proc Natl Acad Sci U S A 2007;104:10364–10369. [PubMed: 17563356]

Spencer S, Dowbenko D, Cheng J, Li W, Brush J, Utzig S, Simanis V, Lasky LA. PSTPIP: a tyrosine phosphorylated cleavage furrow-associated protein that is a substrate for a PEST tyrosine phosphatase. J Cell Biol 1997;138:845–860. [PubMed: 9265651]

Takeda T, Kawate T, Chang F. Organization of a sterol-rich membrane domain by cdc15p during cytokinesis in fission yeast. Nat Cell Biol 2004;6:1142–1144. [PubMed: 15517003]

Tasto JJ, Carnahan RH, McDonald WH, Gould KL. Vectors and gene targeting modules for tandem affinity purification in Schizosaccharomyces pombe. Yeast 2001;18:657–662. [PubMed: 11329175]

Tsujita K, Suetsugu S, Sasaki N, Furutani M, Oikawa T, Takenawa T. Coordination between the actin cytoskeleton and membrane deformation by a novel membrane tubulation domain of PCH proteins is involved in endocytosis. J Cell Biol 2006;172:269–279. [PubMed: 16418535]

Vallen EA, Caviston J, Bi E. Roles of Hof1p, Bni1p, Bnr1p, and myo1p in cytokinesis in Saccharomyces cerevisiae. Mol Biol Cell 2000;11:593–611. [PubMed: 10679017]

Vavylonis D, Wu JQ, Hao S, O'Shaughnessy B, Pollard TD. Assembly mechanism of the contractile ring for cytokinesis by fission yeast. Science 2008;319:97–100. [PubMed: 18079366]

Wachtler V, Huang Y, Karagiannis J, Balasubramanian MK. Cell cycle-dependent roles for the FCH-domain protein Cdc15p in formation of the actomyosin ring in Schizosaccharomyces pombe. Mol Biol Cell 2006;17:3254–3266. [PubMed: 16687577]

Wang Q, Navarro MV, Peng G, Molinelli E, Lin Goh S, Judson BL, Rajashankar KR, Sondermann H. Molecular mechanism of membrane constriction and tubulation mediated by the F-BAR protein Pacsin/Syndapin. Proc Natl Acad Sci U S A 2009;106:12700–12705. [PubMed: 19549836]

Wolfe BA, Gould KL. Split decisions: coordinating cytokinesis in yeast. Trends Cell Biol 2005;15:10–18. [PubMed: 15653073]

Wu JQ, Kuhn JR, Kovar DR, Pollard TD. Spatial and temporal pathway for assembly and constriction of the contractile ring in fission yeast cytokinesis. Dev Cell 2003;5:723–734. [PubMed: 14602073]

Wu JQ, Pollard TD. Counting cytokinesis proteins globally and locally in fission yeast. Science 2005;310:310–314. [PubMed: 16224022]

Wu JQ, Sirotkin V, Kovar DR, Lord M, Beltzner CC, Kuhn JR, Pollard TD. Assembly of the cytokinetic contractile ring from a broad band of nodes in fission yeast. J Cell Biol 2006;174:391–402. [PubMed: 16864655]

Wu X, Gan B, Yoo Y, Guan JL. FAK-mediated src phosphorylation of endophilin A2 inhibits endocytosis of MT1-MMP and promotes ECM degradation. Dev Cell 2005;9:185–196. [PubMed: 16054026]

Wu Y, Spencer SD, Lasky LA. Tyrosine phosphorylation regulates the SH3-mediated binding of the Wiskott-Aldrich syndrome protein to PSTPIP, a cytoskeletal-associated protein. J Biol Chem 1998;273:5765–5770. [PubMed: 9488710]

Yaffe MB, Rittinger K, Volinia S, Caron PR, Aitken A, Leffers H, Gamblin SJ, Smerdon SJ, Cantley LC. The structural basis for 14-3-3:phosphopeptide binding specificity. Cell 1997;91:961–971. [PubMed: 9428519]

Yonetani A, Lustig RJ, Moseley JB, Takeda T, Goode BL, Chang F. Regulation and Targeting of the Fission Yeast Formin cdc12p in Cytokinesis. Mol Biol Cell 2008;19:2208–2219. [PubMed: 18305104]

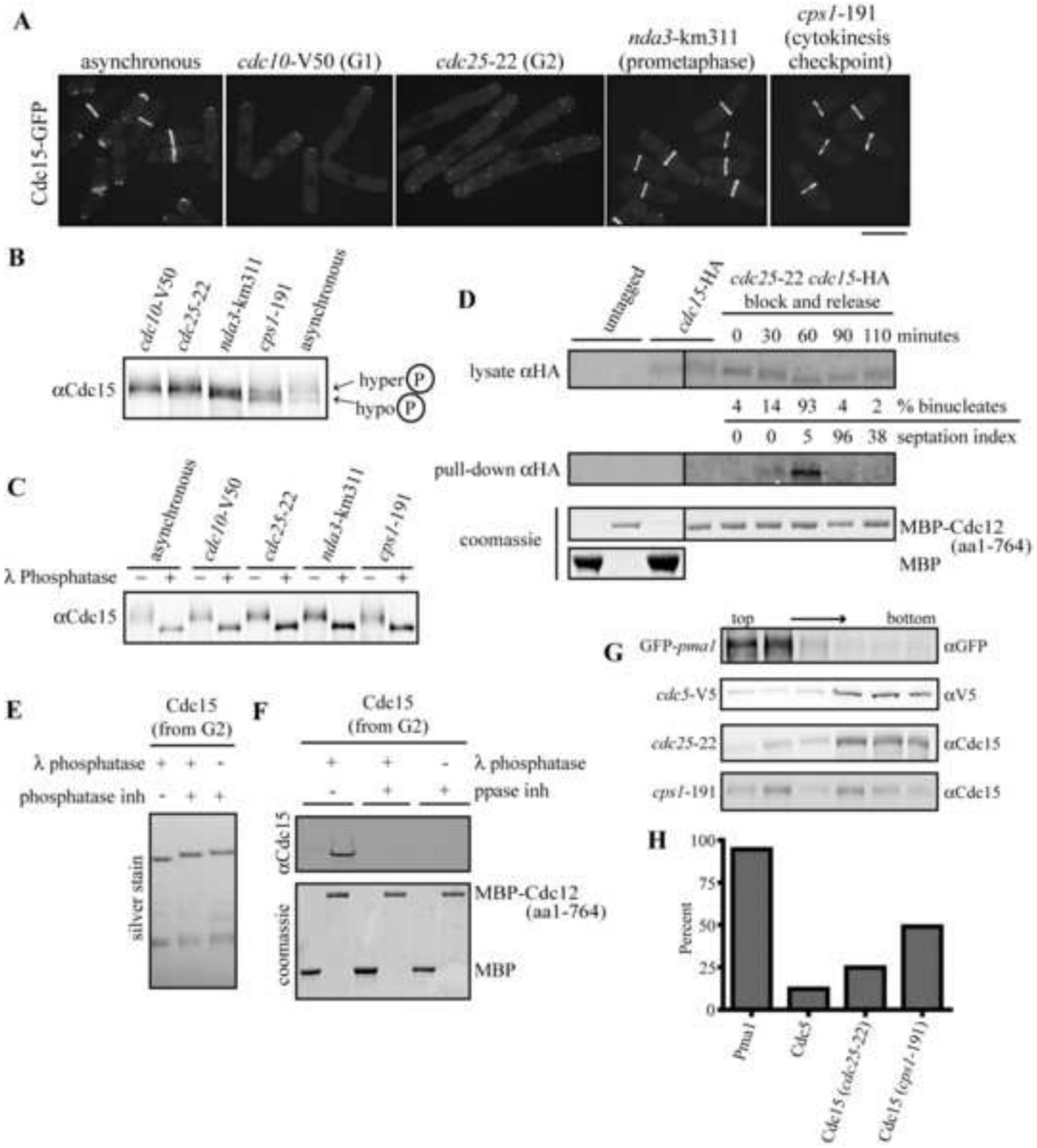

Figure 1. Dephosphorylated Cdc15 binds Cdc12 and localizes to the contractile ring

A) Live cell imaging of the indicated strains grown asynchronously or after the indicated arrest. B) Denatured cell lysates were prepared from the indicated strains and probed with anti-Cdc15 serum. C) Cdc15 was immunoprecipitated from denatured cell lysates and subjected either to lambda phosphatase treatment or a buffer control prior to immunoblotting. D) Block and release of *cdc25-22 cdc15-HA* cells. At the indicated time points, cell cycle progression was monitored by septation index and percentage of binucleate cells. Cell pellets from each time point were subjected to native lysis. Lysates were probed with either bead-bound, recombinant MBP or MBP-Cdc12(aa1-764). Lysate samples and bound proteins were run on SDS-PAGE and Cdc15 was detected by an anti-HA antibody. E)

Hyperphosphorylated Cdc15 was purified and subjected to lambda phosphatase treatment, phosphatase plus inhibitors, or buffer controls. Samples were run on SDS-PAGE and detected by silver staining. F) The Cdc15 purified in E was incubated with bead-bound MBP or MBP-Cdc12(aa1-764). Bound Cdc15 was detected by immunoblotting. G) Lysates of the indicated genotypes were subjected to membrane flotation. Fractions were taken for detection of proteins by immunoblotting. H) Quantitation of the amount of protein in G for the top three fractions of each sample. Bar: (A) 10 μm.

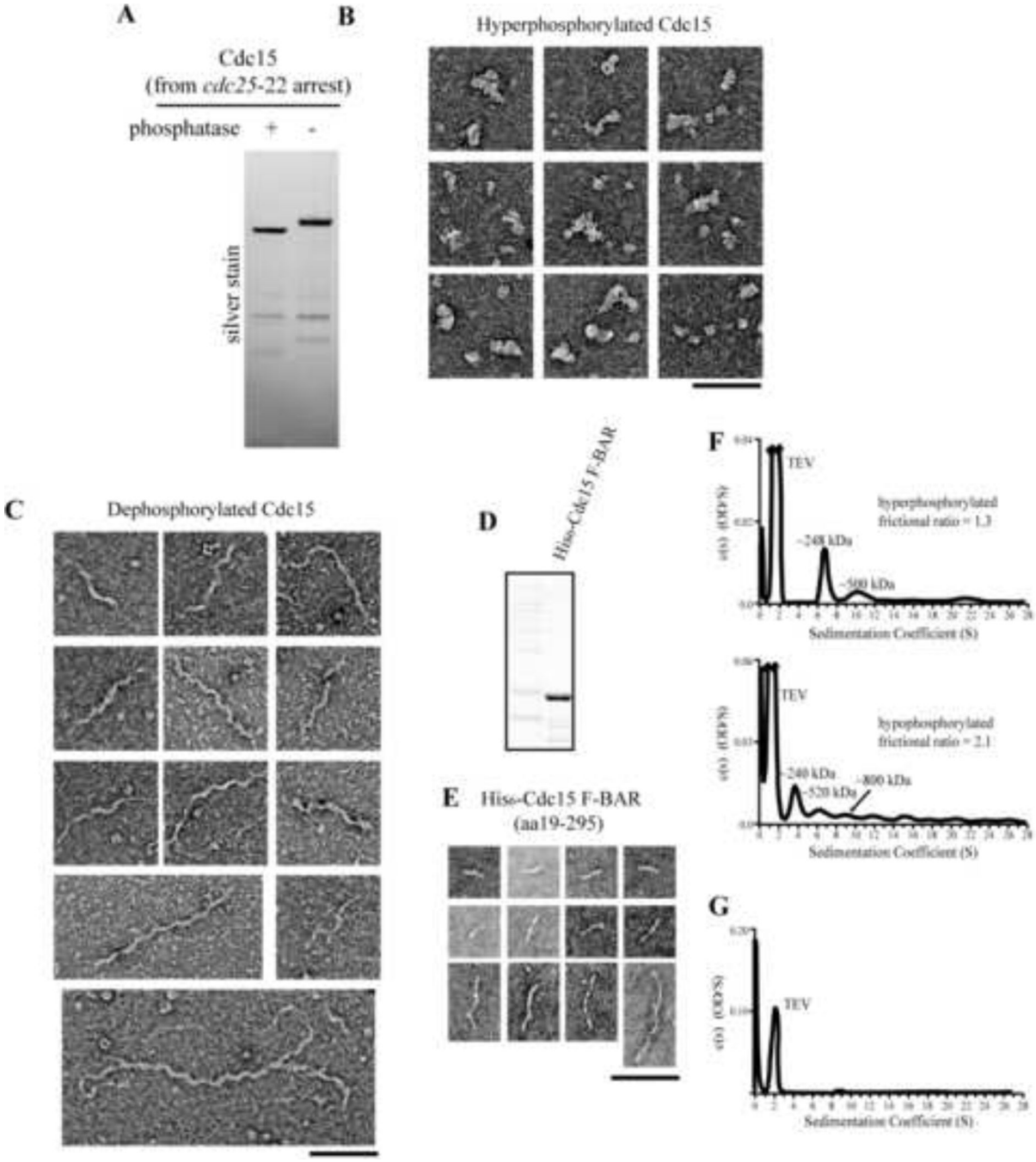

Figure 2. Dephosphorylation of Cdc15 induces conformational and oligomeric changes

A) Hyperphosphorylated Cdc15 was purified, treated with lambda phosphatase or a buffer control, and run on SDS-PAGE. B) Representative negative stain EM images of Cdc15 after treatment with buffer control. C) Representative negative stain EM images of Cdc15 after treatment with lambda phosphatase. Filaments were heterogeneous in length but always contained series of undulating curves. D) His_6-Cdc15 F-BAR was purified and run on SDS-PAGE for detection by coomassie staining. E) Representative EM images of His_6-Cdc15 F-BAR. F) Analytical ultracentrifugation traces of Cdc15 purified in its hyper- and hypophosphorylated forms. TEV contaminant is marked. G) TEV run alone for comparison to F. Bars: 100 nm.

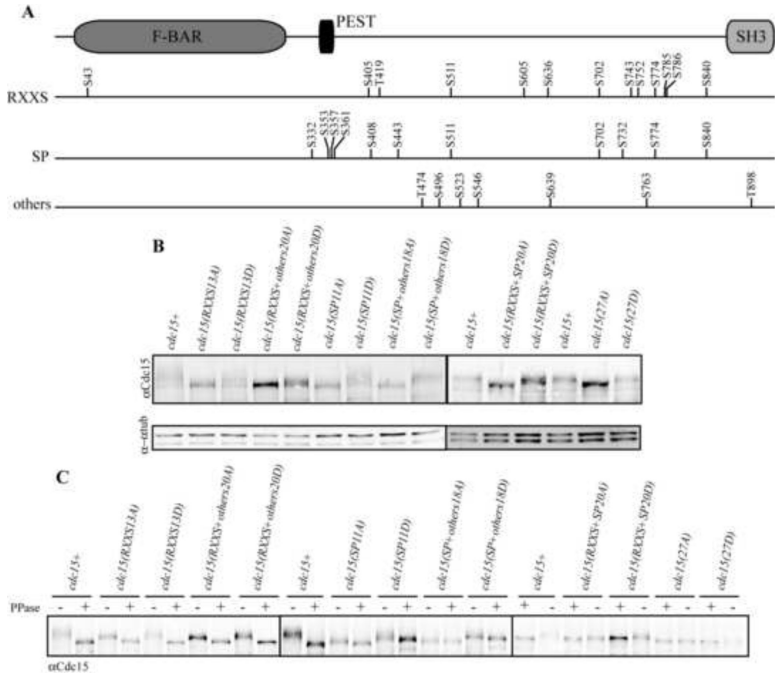

Figure 3. Identification of Cdc15 phosphosites

A) Schematic of phosphorylation mutants. B) Cell lysates were prepared and run on SDS-PAGE. Cdc15 was detected by anti-Cdc15 serum and alpha-tubulin was detected with a DM1a antibody as a loading control. C) Wild type or mutant Cdc15 proteins were immunoprecipitated with anti-Cdc15 serum, subjected to lambda phosphatase treatment or buffer control, and detected by immunoblotting.

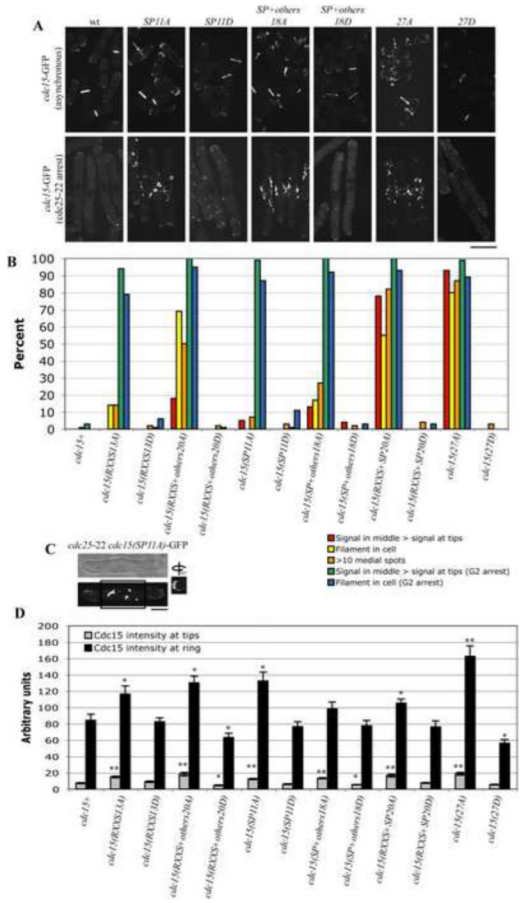

Figure 4. Cdc15 alanine mutants display precocious medial localization

A) Above, live cell imaging of asynchronous cells expressing endogenously-tagged wild type or mutant Cdc15. Arrows indicate medial localization and asterisks indicate filament-like GFP structures. Below, *cdc25*-22 cells with the indicated GFP-tagged *cdc15* mutations were arrested and imaged live. B) Quantitation of images of cells of the indicated genotypes from A. C) A reconstruction of the cell middle of an arrested *cdc25*-22 *cdc15(SP11A)*-GFP cell (marked with the box) was rotated 90°. D) Wild type and mutant Cdc15-GFP intensity was measured and averaged for 15 cells per genotype. Bars are S.E.M. $P<0.05$ (*) or $P<0.001$ (**). Bars: (A) 10 μm, (C) 5 μm.

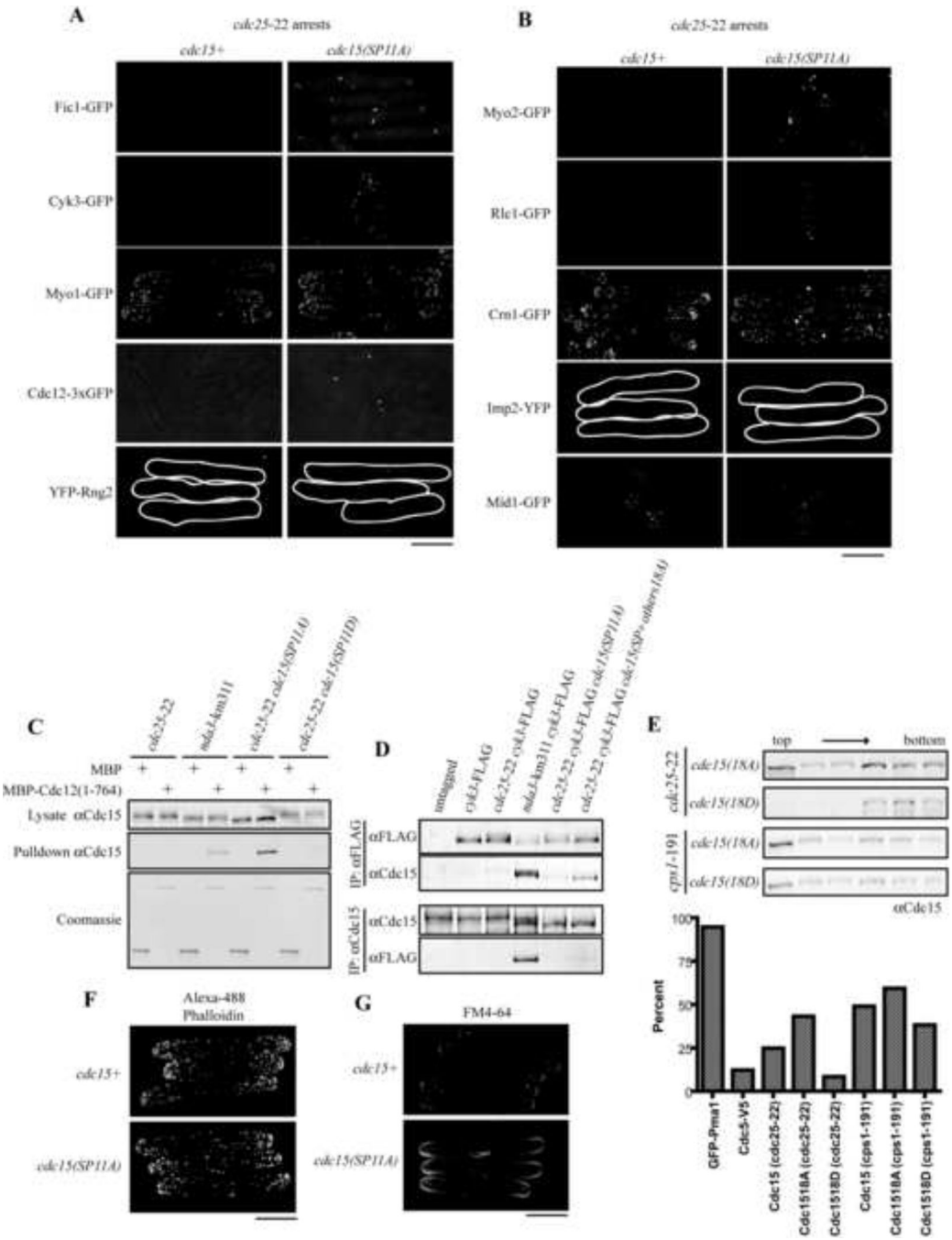

Figure 5. Effects of Cdc15 alanine mutants on other contractile ring components

A and B) *cdc25*-22 or *cdc25*-22 *cdc15(SP11A)* cells expressing the indicated GFP- or YFP-tagged proteins were arrested and imaged. C) Native lysates were probed with MBP or MBP-Cdc12(1-764) and Cdc15 was detected in cell lysates and pull down samples by immunoblotting. D) Native cell lysates were prepared from cells of the indicated genotypes/arrests. Co-immunoprecipitation of Cdc15 with Cyk3 or vice versa was determined by immunoblotting with anti-Cdc15 serum or an anti-FLAG antibody. E) Lysates were prepared for the indicated genotypes and arrests and used for membrane flotation as in Fig. 1G–H. F) *cdc25*-22 or *cdc25*-22 *cdc15(SP11A)* cells were arrested, fixed, and stained with Alexa Fluor-488 phalloidin for confocal imaging. G) *cdc25*-22 or *cdc25*-22 *cdc15(SP11A)*

cells were grown to log phase, arrested, exposed to FM4-64 and immediately imaged live. Bars: 10 μm.

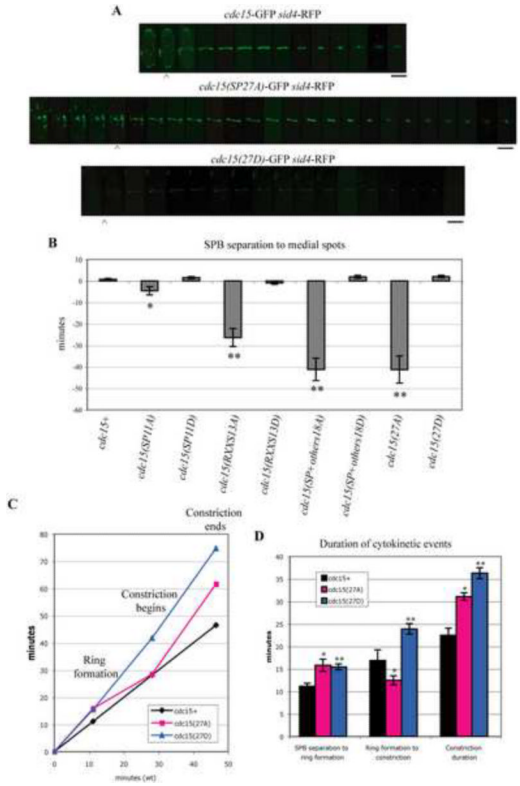

Figure 6. Altered dynamics in Cdc15 alanine mutants

A) *cdc15*-GFP, *cdc15(27A)*-GFP, or *cdc15(27D)*-GFP cells with *sid4*-RFP were grown to log phase, synchronized with a lactose gradient, and imaged by time lapse microscopy. Montages for each genotype were assembled from movies (images at 5 minute intervals). Ectopic spots are visible in the *cdc15(SP27A)*-GFP mutant. SPB separation is denoted in each movie with a carat. B) Quantitation of spot appearance before SPB separation in each indicated mutant (n>10 for each). Asterisks denote P ≤0.01 (*) or ≤0.001 (**). C and D) Quantitation of cytokinesis event timing for phosphorylation mutants from A (n>10 for each). Asterisks denote P ≤0.05 (*) or ≤0.001 (**). Error bars represent S.E.M. Bars: 5 μm.

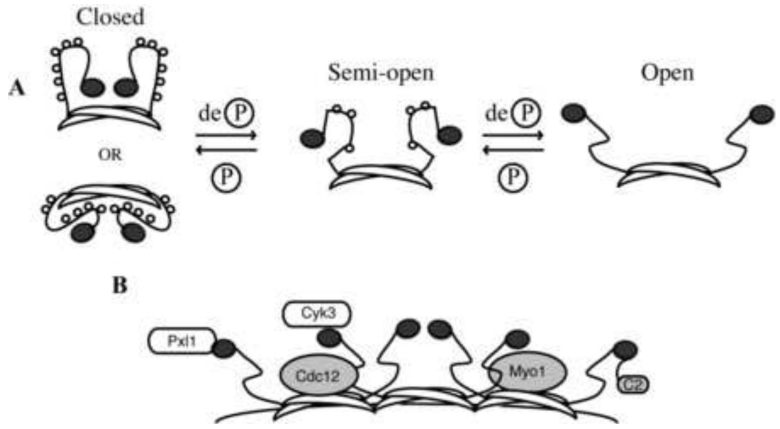

Figure 7. Model for Cdc15 phosphoregulation

A) Model for alteration of Cdc15 conformation by phosphorylation and dephosphorylation. B) Depiction of hypophosphorylated Cdc15 in its active scaffolding role at the contractile ring.